

Improved many-electron wavefunctions from plasmon normal modes

B Wood and W M C Foulkes

Blackett Laboratory, Imperial College, Prince Consort Road, London SW7 2BW, UK

E-mail: ben.wood@imperial.ac.uk

Received 20 October 2005, in final form 5 January 2006

Published 3 February 2006

Online at stacks.iop.org/JPhysCM/18/2305

Abstract

We investigate an alternative approach to the connection between plasmons and the ground-state wavefunction of many-electron systems, starting with a classical plasmon Hamiltonian. We obtain a prescription for the part of the wavefunction which determines the long-ranged electron–electron correlations; we then show how this prescription can be used to construct improved trial wavefunctions for use in quantum Monte Carlo simulations.

Using the quasi-2D electron gas as a test system, we construct a trial wavefunction of the Slater–Jastrow form, combining mean-field single-electron orbitals with short-ranged and plasmon-derived long-ranged correlations. Variational quantum Monte Carlo calculations show that the new wavefunction reduces the expectation value of the energy, but the short-ranged correlations are more important than the plasmon-derived ones. Finally, we present a computationally efficient Jastrow factor, which we recommend for future simulations.

(Some figures in this article are in colour only in the electronic version)

1. Introduction

It has long been known that there is a connection between the collective charge oscillations known as plasmons and the ground-state wavefunction of many-electron systems [1]. In this paper, we aim to clarify this connection.

The motivation for this work is the need for good trial wavefunctions in our quantum Monte Carlo (QMC) simulations. The term ‘quantum Monte Carlo’ groups together many different techniques that involve using Monte Carlo methods to solve problems in quantum mechanics [2]. QMC is commonly used to investigate the ground-state of many-electron systems; in this area, the two most popular versions of QMC are variational and fixed-node diffusion Monte Carlo (VMC and DMC) [3]. Both of these methods rely on having a good estimate of the ground-state wavefunction in advance.

Conventionally, the many-electron trial wavefunction takes the form

$$\Psi_T(\mathbf{X}) = e^{J(\mathbf{X})} D(\mathbf{X}) \quad (1)$$

where \mathbf{X} represents all the electron spins and positions, D is a determinant made up of single-electron orbitals, and e^J is a totally symmetric function called the Jastrow factor. The quality of the single-electron orbitals sets a hard limit on the accuracy of VMC and DMC simulations. The Jastrow factor cannot alter the position of the nodes, and therefore cannot improve the fixed-node DMC energy; however, a good Jastrow factor significantly improves both the ground-state energy in VMC and the efficiency of fixed-node DMC simulations. In certain circumstances, a poor-quality Jastrow factor can make DMC simulations impossible, because the consequent population fluctuations become unmanageable. It is thus very important to obtain as much information as possible about the correct form of the wavefunction by analytical means. One way to obtain a better Jastrow factor is through a consideration of plasmons [4].

In a system with a homogeneous electron density, plasmons are well defined for wavelengths above some critical value; for wavelengths below this value, the plasmons are able to decay to form electron–hole pairs. The existence of long-lived plasmons suggests that we should be able to separate the full many-electron Hamiltonian into a plasmon part and a screened part. If we ignore the coupling between the two, we can approximate the ground-state wavefunction as a product of a plasmon term and a screened term. It turns out that the plasmon term naturally provides a significant part of the Jastrow factor. Several authors have studied this relationship for homogeneous [1] and inhomogeneous [5] systems.

Here, we present a prescription for obtaining a Jastrow factor for general inhomogeneous systems that is consistent with the previous work, although based on a more ‘physical’ approach; in addition, we show how a knowledge of the classical plasmon normal modes allows an alternative method for writing down J .

We then apply this method to our test system—the quasi-2D electron gas. In doing so, we illustrate some of the technical challenges involved in constructing a practical Jastrow factor, and introduce a new term to deal with short-range correlations. The results of our VMC simulations demonstrate the effect of the new Jastrow factor on the electron density and on the energy expectation value. We find that using the full plasmon Jastrow factor reduces the energy expectation value, although not significantly more than using only the short-ranged term.

The plasmon Jastrow exponent includes terms which correlate the motion of pairs of electrons (usually denoted u), as well as single-electron terms that act to modify the electron density (denoted χ). The relationship between the two is of the form proposed by Malatesta *et al* [6], namely

$$\chi(\mathbf{r}) = \int_{\Omega} \bar{n}(\mathbf{r}') u(\mathbf{r}, \mathbf{r}') d^3 r' \quad (2)$$

where \bar{n} is the electron density. We use the same relationship when constructing the part of the Jastrow factor that deals with short-range correlations (which is not related to plasmons); we choose a form for u , and then calculate χ using the formula (2). The resulting Jastrow factor performs very well, and is computationally inexpensive. This approach has the advantage of reducing the number of parameters in the Jastrow factor, since χ is completely determined once u has been chosen. Of course, additional terms can subsequently be included in χ if required. It is normal to parametrize the Jastrow factor in a flexible way, and then to optimize the parameters; we find that calculating χ from u can significantly improve the efficiency of this procedure.

2. The plasmon Hamiltonian

Our first task is to write down a classical Hamiltonian for our system, which consists of a gas of electrons moving in some time-independent background potential ϕ_b . The hydrodynamic kinetic energy of this gas is

$$T = \frac{1}{2} \int_{\Omega} n(\mathbf{r}, t) m_e |\mathbf{v}(\mathbf{r}, t)|^2 d^3r \quad (3)$$

where n is the electron number density and \mathbf{v} is the hydrodynamical velocity. We work in the electrostatic approximation, neglecting magnetic interactions and relativistic effects; we can therefore write the potential energy as

$$V = \int_{\Omega} en(\mathbf{r}, t) \left[-\phi_b(\mathbf{r}) + \frac{1}{2} \int_{\Omega} \frac{en(\mathbf{r}', t)}{4\pi\epsilon_0|\mathbf{r}-\mathbf{r}'|} d^3r' \right] d^3r. \quad (4)$$

The potential energy is minimized when the total charge density of the system is uniformly zero. We can use this condition, or simply take the variation of the potential energy with respect to n to show that the required electron density is \bar{n} , where

$$\phi_b(\mathbf{r}) = \int_{\Omega} \frac{e\bar{n}(\mathbf{r}')}{4\pi\epsilon_0|\mathbf{r}-\mathbf{r}'|} d^3r'. \quad (5)$$

The kinetic energy can be simultaneously minimized by requiring that $\mathbf{v} = \mathbf{0}$. Of course, n and \mathbf{v} are not independent, but when $n = \bar{n}$ there is no net force on the electron gas and $\mathbf{v} = \mathbf{0}$ is an acceptable solution.

A plasmon is a small oscillation about the ground-state density. We therefore write

$$n(\mathbf{r}, t) = \bar{n}(\mathbf{r}) - \frac{\rho(\mathbf{r}, t)}{e} \quad (6)$$

where ρ is the change in the charge density associated with the plasmon; this is assumed to be small, along with all other time-dependent quantities, including \mathbf{v} .

We can write our Hamiltonian as the sum of kinetic and potential energies, expanded around $n = \bar{n}$:

$$H = T + V = \frac{1}{2} \int_{\Omega} \bar{n}(\mathbf{r}) m_e |\mathbf{v}(\mathbf{r}, t)|^2 d^3r' + \frac{1}{2} \int_{\Omega} \int_{\Omega} \frac{\rho(\mathbf{r}, t) \rho(\mathbf{r}', t)}{4\pi\epsilon_0|\mathbf{r}-\mathbf{r}'|} d^3r' d^3r \\ - \underbrace{\frac{1}{2} \int_{\Omega} \frac{\rho(\mathbf{r}, t) m_e |\mathbf{v}(\mathbf{r}, t)|^2}{e} d^3r}_{\text{higher-order}} - \underbrace{\frac{1}{2} \int_{\Omega} \int_{\Omega} \frac{e^2 \bar{n}(\mathbf{r}) \bar{n}(\mathbf{r}')}{4\pi\epsilon_0|\mathbf{r}-\mathbf{r}'|} d^3r' d^3r}_{\text{constant}}. \quad (7)$$

Omitting the constant and third-order terms gives us the desired plasmon Hamiltonian:

$$H = \frac{1}{2} \int_{\Omega} \epsilon_0 \omega_p^2(\mathbf{r}) |\nabla f(\mathbf{r}, t)|^2 d^3r' + \frac{1}{2} \int_{\Omega} \int_{\Omega} \frac{\rho(\mathbf{r}, t) \rho(\mathbf{r}', t)}{4\pi\epsilon_0|\mathbf{r}-\mathbf{r}'|} d^3r' d^3r. \quad (8)$$

Two new variables have been introduced; the first is the position-dependent plasma frequency

$$\omega_p(\mathbf{r}) = \sqrt{\frac{e^2 \bar{n}(\mathbf{r})}{m_e \epsilon_0}}. \quad (9)$$

In a homogeneous gas of density \bar{n} , bulk plasmon oscillations are supported at this frequency (in the simple classical model).

Secondly, we have chosen to write the velocity as the gradient of a scalar field:

$$\mathbf{v}(\mathbf{r}, t) = \frac{e}{m_e} \nabla f(\mathbf{r}, t). \quad (10)$$

This is permitted because the flow is irrotational; the small perturbations to the stationary ground state are caused by the Coulomb force, which cannot induce rotation. We must now determine the relationship between \mathbf{v} and ρ . The force on any infinitesimal volume element of our fluid comes from the electrostatic interaction of that element with the surroundings; since our fluid is made up of electrons, we have

$$m_e \dot{\mathbf{v}} = e \nabla \phi, \quad (11)$$

where the time-dependent electrostatic potential is

$$\phi(\mathbf{r}, t) = \int_{\Omega} \frac{\rho(\mathbf{r}', t)}{4\pi\epsilon_0|\mathbf{r} - \mathbf{r}'|} d^3r'. \quad (12)$$

This is the total potential: the contributions from the background and the equilibrium electron density do not appear because they cancel exactly. We have ignored the pressure in the fluid.

The Hamiltonian (8) is written in terms of the fields f and ρ , which we will show below to be mutually conjugate. The corresponding canonical equations are

$$\dot{f} = \frac{\delta H}{\delta \rho} = \phi \quad (13)$$

$$\dot{\rho} = -\frac{\delta H}{\delta f} = -\nabla \cdot \mathbf{J}. \quad (14)$$

The first of these ensures that (11) is satisfied; the second is the equation of continuity, with the current density

$$\mathbf{J} = -\bar{n}e\mathbf{v}. \quad (15)$$

We have used the definitions (9), (10), and (12).

Our approach began with the formulation of a Hamiltonian. It is more conventional to start with a Lagrangian, expressed in terms of the derivatives of a single field; the conjugate field can then be defined, and a Legendre transformation leads to the Hamiltonian. Our physically motivated Hamiltonian can be derived from the following Lagrangian¹:

$$L = \frac{1}{2}\epsilon_0 \int_{\Omega} \left[-\omega_p^2(\mathbf{r}) |\nabla f(\mathbf{r}, t)|^2 + |\nabla \dot{f}(\mathbf{r}, t)|^2 \right] d^3r. \quad (16)$$

We can now confirm that the charge density and the velocity potential are conjugate variables:

$$\frac{\delta L}{\delta \dot{f}} = -\epsilon_0 \nabla^2 \dot{f} = \rho. \quad (17)$$

The Legendre transformation

$$H = \int_{\Omega} \rho(\mathbf{r}, t) \dot{f}(\mathbf{r}, t) d^3r - L \quad (18)$$

then gives the Hamiltonian described in (8).

Quantization proceeds by letting f and ρ become operators, subject to the commutation relation

$$\left[\hat{f}(\mathbf{r}), \hat{\rho}(\mathbf{r}') \right] = i\hbar \delta(\mathbf{r} - \mathbf{r}'). \quad (19)$$

¹ The reason for writing the Lagrangian in terms of f and \dot{f} , and hence making f into the 'position' variable (rather than ρ , which would usually be the natural choice), is that the kinetic energy term cannot easily be expressed in terms of $\dot{\rho}$.

3. Normal modes

To find the ground-state wavefunction, we can write the plasmon Hamiltonian using the normal mode amplitudes as variables. It will then be reduced to a form corresponding to a set of independent oscillators, and we will be able to write down the ground-state wavefunction.

The equation of motion for the electrostatic potential is obtained by combining the canonical equations (13) and (14) with the definitions (9), (10), (12) and (15):

$$-\nabla^2 \ddot{\phi} = \nabla \cdot (\omega_p^2 \nabla \phi). \quad (20)$$

The velocity potential satisfies the same equation; working with ϕ rather than f is therefore a matter of choice. On the other hand, we do not work with the charge density because the relevant equation of motion is less tractable.

The defining characteristic of a normal mode is harmonic time dependence; the normal modes of the electrostatic potential therefore satisfy the equation

$$\omega_i^2 \nabla^2 \phi_i = \nabla \cdot (\omega_p^2 \nabla \phi_i). \quad (21)$$

Assuming appropriate boundary conditions, the solutions of this equation are orthogonal, in the sense that

$$\int_{\Omega} \nabla \phi_i \cdot \nabla \phi_j \, d^3 r = \delta_{ij}, \quad (22)$$

where we have chosen the normalization. The modes are also orthogonal when weighted with the local plasma frequency:

$$\int_{\Omega} \omega_p^2 \nabla \phi_i \cdot \nabla \phi_j \, d^3 r = \omega_i^2 \delta_{ij}. \quad (23)$$

These properties follow from (20), and the use of physical boundary conditions.

The canonical transformation to the normal coordinates $\{\alpha_i\}$ and $\{\beta_i\}$ can be achieved with the generating function [7]

$$\Phi = \sum_i \beta_i \int_{\Omega} \nabla \phi_i \cdot \nabla f \, d^3 r. \quad (24)$$

We then have

$$\alpha_i = \frac{\partial \Phi}{\partial \beta_i} = \int_{\Omega} \nabla \phi_i \cdot \nabla f \, d^3 r \quad (25)$$

$$\rho = \frac{\delta \Phi}{\delta f} = - \sum_i \beta_i \nabla^2 \phi_i. \quad (26)$$

Equation (25) shows that α_i is the amplitude of the i th normal mode; the use of the generating function ensures that α_i and β_i are conjugate variables.

We can invert these expressions by using the orthonormality condition (22) to give

$$\nabla f = \sum_i \alpha_i \nabla \phi_i \quad (27)$$

$$\beta_i = \int_{\Omega} \phi_i \rho \, d^3 r. \quad (28)$$

The quantum mechanical operators representing the normal mode amplitudes obey the commutation relation

$$[\hat{\alpha}_i, \hat{\beta}_j] = i\hbar \delta_{ij}, \quad (29)$$

as can be verified by substitution. If the normal modes are chosen to be real, the operators $\{\hat{\alpha}_i\}$ and $\{\hat{\beta}_i\}$ are Hermitian.

Using the normal coordinates, the Hamiltonian operator becomes

$$\hat{H} = \frac{1}{2} \sum_i \left(\frac{1}{\epsilon_0} \hat{\beta}_i^2 + \epsilon_0 \omega_i^2 \hat{\alpha}_i^2 \right). \quad (30)$$

Given this simple form, we can immediately write down the ground-state wavefunction in the β_i -representation:

$$\Psi_{\text{pl}}(\{\beta_i\}) = \exp \left(-\frac{1}{2\epsilon_0 \hbar} \sum_i \frac{1}{\omega_i} \beta_i^2 \right), \quad (31)$$

or, using (6) and (28), we can write it in terms of the electron density:

$$\Psi_{\text{pl}}[n] = \exp \left\{ -\frac{e^2}{2\epsilon_0 \hbar} \sum_i \frac{1}{\omega_i} \left[\int_{\Omega} \phi_i (n - \bar{n}) \, d^3r \right]^2 \right\}. \quad (32)$$

We would like to express the wavefunction in terms of the electron coordinates $\{\mathbf{r}_i\}$. To this end, we will use the definition of the electron density

$$n(\mathbf{r}) = \sum_i \delta(\mathbf{r} - \mathbf{r}_i) \quad (33)$$

to substitute for n . However, we must be careful. We have not derived the full ground-state wavefunction for a many-electron system here; we have only calculated that part which determines long-range correlations and gives rise to long-wavelength collective charge oscillations. Thus, we may write

$$\Psi_{\text{pl}}(\{\mathbf{r}_i\}) = \exp \left[-\frac{1}{2} \sum_{i,j} u_{\text{pl}}(\mathbf{r}_i, \mathbf{r}_j) + \sum_i \chi_{\text{pl}}(\mathbf{r}_i) \right] \quad (34)$$

where

$$\chi_{\text{pl}}(\mathbf{r}) = \frac{e^2}{\epsilon_0 \hbar} \sum_i \frac{1}{\omega_i} \phi_i(\mathbf{r}) \int_{\Omega} \phi_i(\mathbf{r}') \bar{n}(\mathbf{r}') \, d^3r' \quad (35)$$

and

$$u_{\text{pl}}(\mathbf{r}, \mathbf{r}') = \frac{e^2}{\epsilon_0 \hbar} \sum_i \frac{1}{\omega_i} \phi_i(\mathbf{r}) \phi_i(\mathbf{r}'), \quad (36)$$

as long as we understand that we are dealing with only part of the full many-electron wavefunction.

The two-body term, u_{pl} , correlates the motion of pairs of electrons. In a homogeneous system, where the normal modes are plane waves oscillating at the plasma frequency, it becomes

$$u_{\text{pl}}^{\text{hom}}(\mathbf{r}, \mathbf{r}') = \frac{e^2}{4\pi \epsilon_0 \hbar \omega_p |\mathbf{r} - \mathbf{r}'|} \quad (37)$$

as expected [1].

The plasmon theory also generates a one-body term, χ_{pl} . This can be thought of as ‘density restoring’: it ensures that the electron density does not deviate much from \bar{n} , as it would if only the two-body term were present.

4. Constructing the many-electron wavefunction

Plasmons are long-wavelength oscillations. In a homogeneous system with electron density $(\frac{4}{3}\pi r_s^3)^{-1}$, plasmons with a wavevector greater than

$$k_c \approx \frac{1}{\sqrt{r_s}} \quad (38)$$

are no longer well defined: they are able to decay to form electron–hole pairs [8, 9]. Although the situation is less clear when the system is inhomogeneous, there will still be a cut-off; this means that the expressions derived above will only provide the long-range correlations between electrons.

The full electronic Hamiltonian contains the kinetic energy and the Coulomb interaction terms; the plasmon Hamiltonian contains only the long-wavelength components of the Coulomb interaction. In effect, we have separated the Schrödinger equation, based on the physical observation that plasmons exist, and have long lifetimes:

$$\hat{H} \approx \hat{H}_{\text{pl}} + \hat{H}_{\text{red}}. \quad (39)$$

We neglect the weak coupling between the two terms. The remaining non-plasmonic part of the Hamiltonian, \hat{H}_{red} , includes the usual short-wavelength interactions, but the long-wavelength interactions are screened: only a mean-field picture remains, since the fluctuations around this mean field make up the plasmons.

The full ground-state wavefunction can therefore be approximated by a product of two terms:

$$\Psi_0 \approx \Psi_{\text{pl}}\Psi_{\text{red}}, \quad (40)$$

where Ψ_{red} is the ground state of the reduced Hamiltonian operator (with the long-wavelength interactions treated in a mean-field way).

We can compare this approximation with the Slater–Jastrow wavefunction conventionally used in QMC simulations (1). The plasmon ground-state wavefunction Ψ_{pl} is exponential in form, and so makes up part of the Jastrow factor. If we combine a Slater determinant composed of single-electron orbitals obtained from a mean-field (density-functional or Hartree–Fock theory) calculation with a Jastrow factor which includes only short-range correlations, then we have an approximation to Ψ_{red} . We still need to determine the form of the short-range correlations, but for this we can appeal to Kato’s cusp conditions [10].

Our approximation to the ground-state wavefunction is therefore of the conventional Slater–Jastrow type, with the following Jastrow exponent:

$$J = -\frac{1}{2} \sum_{i,j} [u_{\text{pl}}(\mathbf{r}_i, \mathbf{r}_j) + u_{\text{cusp}}(\mathbf{x}_i, \mathbf{x}_j)] + \sum_i [\chi_{\text{pl}}(\mathbf{r}_i) + \chi_{\text{cusp}}(\mathbf{r}_i)]. \quad (41)$$

The function u_{cusp} should give the correct gradient discontinuity when the two relevant electrons lie on top of one another, and should tend to a constant when they are far apart (so that the plasmon term then dominates). The separation distance which marks the crossover between these two regimes should be of the order of k_c^{-1} . We choose the function

$$u_{\text{cusp}}(\mathbf{x}_i, \mathbf{x}_j) = \left(\frac{m_e e^2}{4\pi \epsilon_0 \hbar^2} \right) \frac{1}{2k_c} \left(\frac{1}{1 + \delta_{\sigma_i \sigma_j}} \right) \exp \left(-k_c r_{ij} - \frac{r_{ij}^2}{L_c^2} \right). \quad (42)$$

The Gaussian damping term has been included to avoid creating unwanted cusps in the wavefunction for periodic systems; the parameter L_c is set to ensure that u_{cusp} is very small when r_{ij} approaches the size of the simulation cell.

The introduction of u_{cusp} will change the electron density of an inhomogeneous system. Generally, electrons will be pushed further apart, causing regions of high density to spread out: the inhomogeneity of the system is reduced. Fahy and co-workers [11] were the first to point out in the context of QMC simulations that adding a homogeneous² two-body term causes the electron density to become more uniform. We have seen that the plasmon theory generates a one-body term, χ_{pl} ; this compensates for the change in the electron density which would otherwise be brought about by u_{pl} . A similar compensatory term is required to go with u_{cusp} ; we have therefore included χ_{cusp} .

A comparison of the definitions of u_{pl} (36) and χ_{pl} (35) shows that they are related as follows:

$$\chi_{\text{pl}}(\mathbf{r}) = \int_{\Omega} \bar{n}(\mathbf{r}') u_{\text{pl}}(\mathbf{r}, \mathbf{r}') d^3 r'. \quad (43)$$

A relationship of this form between the one- and two-body terms in the Jastrow factor was postulated by Malatesta *et al* [6], based on a plausibility argument. We will apply the same principle in this work to calculate the density-correcting term corresponding to u_{cusp} ; in other words, we set

$$\chi_{\text{cusp}}(\mathbf{r}) = \int_{\Omega} \bar{n}(\mathbf{r}') u_{\text{cusp}}(\mathbf{r}, \mathbf{r}') d^3 r'. \quad (44)$$

In the following sections, we will test the effectiveness of this construction, along with the other components of our Jastrow factor, by applying our method to a test system: the quasi-2D electron gas. This will also provide a demonstration of the process involved in creating the wavefunction.

5. The quasi-2D electron gas

The quasi-2D electron gas consists of a gas of electrons moving in the potential provided by a fixed background of positive charge. The background charge density is uniform, with infinite extent in the xy -plane but finite extent in the z -direction. The number of electrons per unit area (in the xy -plane) is determined by the requirement that the system be charge neutral, and therefore depends on the density of the background charge and on the slab width. Our simulation cell will consist of a square of side L in the xy -plane, with infinite extent in the z -direction.

Usually, the electrons are allowed to spill into the vacuum region, outside the fixed background; this system is conventionally referred to as the jellium slab. It is also possible to confine the system further, by imposing infinite potential barriers at the slab edges: this is known as the infinite barrier model. We will test both systems here.

5.1. Plasmon modes

The first task is to determine the plasmon normal modes. We choose our coordinate system so that the upper and lower surfaces of the slab are at $z = 0$ and s ; for the purpose of calculating the normal modes, we will assume that the electron density (and hence the plasma frequency) is constant inside the slab and zero outside. Applying this assumption to the normal mode equation (21) shows that outside the slab the normal modes are solutions of Laplace's equation:

$$\nabla^2 \phi_i = 0 \quad (z < 0, z > s) \quad (45)$$

² The term 'homogeneous' here refers to the fact that u only depends on the relative spin and separation of the electrons, and not on their individual positions, as is appropriate in a system of uniform electron density.

while inside the slab, we have

$$\left(\omega_i^2 - \omega_p^2\right) \nabla^2 \phi_i = 0 \quad (0 < z < s). \quad (46)$$

From now on, we will use ω_p to denote the constant plasma frequency within the slab.

The boundary conditions at $z = 0$ and s can be obtained in the standard way [12]. We integrate the normal mode equation (21) over an infinitesimal Gaussian pillbox straddling the boundary to show that $\epsilon_r \partial \phi / \partial z$ must be continuous at the interface, where the relative permittivity is

$$\epsilon_r = \begin{cases} 1 & \text{outside the slab} \\ 1 - \frac{\omega_p^2}{\omega^2} & \text{inside the slab.} \end{cases} \quad (47)$$

Integrating the irrotational function $\nabla \phi$ around an infinitesimal Stokesian loop (again straddling the boundary) shows that $\partial \phi / \partial x$ and $\partial \phi / \partial y$ are also continuous. We will impose the additional requirement that the electric field must tend to zero far from the slab.

Since our system is periodic in the xy -plane, we look for solutions with xy -dependence of the form $\cos(\mathbf{k}_{\parallel} \cdot \mathbf{r}_{\parallel})$ or $\sin(\mathbf{k}_{\parallel} \cdot \mathbf{r}_{\parallel})$. In the former case, the field outside the slab is

$$\phi_{\mathbf{k}_{\parallel}} \propto \cos(\mathbf{k}_{\parallel} \cdot \mathbf{r}_{\parallel}) \begin{cases} e^{k_{\parallel} z} & \text{for } z < 0 \\ e^{-k_{\parallel}(z-s)} & \text{for } z > s. \end{cases} \quad (48)$$

A second solution is obtained by replacing $\cos(\mathbf{k}_{\parallel} \cdot \mathbf{r}_{\parallel})$ with $\sin(\mathbf{k}_{\parallel} \cdot \mathbf{r}_{\parallel})$.

We are now able to identify a special case: when $\omega = \omega_p$. The permittivity of the slab becomes zero; the continuity of $\epsilon_r \partial \phi / \partial z$ at the interfaces, combined with form of the generic solution (48), then means that there is no field outside the slab. The remaining interfacial boundary conditions imply that ϕ must tend to zero at $z = 0$ and s , but is otherwise unrestricted within the slab:

$$\phi_{\mathbf{k}}^{1(b)} = \begin{cases} \frac{2}{k\sqrt{L^2 s}} \cos(\mathbf{k}_{\parallel} \cdot \mathbf{r}_{\parallel}) \sin k_z z & \text{for } 0 < z < s \\ 0 & \text{otherwise} \end{cases} \quad (49)$$

$$\phi_{\mathbf{k}}^{2(b)} = \begin{cases} \frac{2}{k\sqrt{L^2 s}} \sin(\mathbf{k}_{\parallel} \cdot \mathbf{r}_{\parallel}) \sin k_z z & \text{for } 0 < z < s \\ 0 & \text{otherwise.} \end{cases} \quad (50)$$

The functions are normalized in accordance with our earlier prescription (22). These oscillations, contained entirely within the slab, are called bulk plasmons.

Away from the plasma frequency, the potential within the slab must also be a solution of Laplace's equation. Applying the boundary conditions then gives

$$\phi_{\mathbf{k}_{\parallel}}^{1(s)\pm}(\mathbf{r}) = \left(\frac{1 \mp e^{-k_{\parallel} s}}{2L^2 k_{\parallel}}\right)^{1/2} \cos(\mathbf{k}_{\parallel} \cdot \mathbf{r}_{\parallel}) \begin{cases} e^{k_{\parallel} z} & \text{for } z < 0 \\ \frac{e^{k_{\parallel} z} \mp e^{-k_{\parallel}(z-s)}}{1 \mp e^{k_{\parallel} s}} & \text{for } 0 < z < s \\ \mp e^{-k_{\parallel}(z-s)} & \text{otherwise} \end{cases} \quad (51)$$

$$\phi_{\mathbf{k}_{\parallel}}^{2(s)\pm}(\mathbf{r}) = \left(\frac{1 \mp e^{-k_{\parallel} s}}{2L^2 k_{\parallel}}\right)^{1/2} \sin(\mathbf{k}_{\parallel} \cdot \mathbf{r}_{\parallel}) \begin{cases} e^{k_{\parallel} z} & \text{for } z < 0 \\ \frac{e^{k_{\parallel} z} \mp e^{-k_{\parallel}(z-s)}}{1 \mp e^{k_{\parallel} s}} & \text{for } 0 < z < s \\ \mp e^{-k_{\parallel}(z-s)} & \text{otherwise.} \end{cases} \quad (52)$$

These are the surface plasmons; the field is most intense at the interfaces, and decays exponentially away from there. There are now four modes for each \mathbf{k}_{\parallel} ; the 'plus' and 'minus'

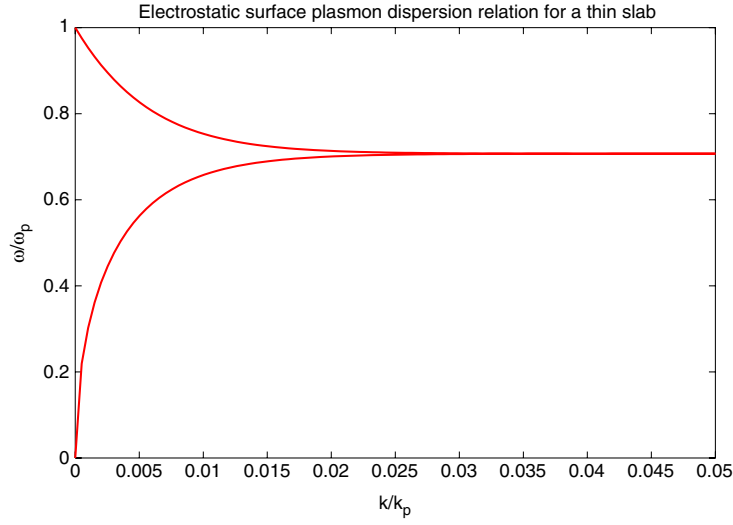


Figure 1. The dispersion relation for surface plasmons in the electrostatic theory. The slab width is 20 au. For metallic densities, the Fermi wavevector is of order unity, whereas $k_p \sim 0.01$. The plasmon frequency very rapidly reaches the large- k limit of $\omega_p/\sqrt{2}$; this is the result obtained for a semi-infinite system.

modes are antisymmetric and symmetric solutions, corresponding to the two branches of the dispersion relation

$$\frac{\omega}{\omega_p} = \sqrt{\frac{1 \pm e^{-ks}}{2}} \quad (53)$$

which was first obtained by Ritchie [13] and is plotted in figure 1. The analysis of surface plasmons in the electrostatic limit was first presented by Ferrell [14]; a more complete treatment, going beyond the electrostatic limit and including quantum mechanical effects, is contained in the work by Boardman [15].

The wavevectors \mathbf{k}_{\parallel} and k_z are subject to several restrictions:

- each \mathbf{k}_{\parallel} is a reciprocal lattice vector of the simulation cell;
- if \mathbf{k}_{\parallel} is included in the set, then $-\mathbf{k}_{\parallel}$ is not;
- $k_z = n\pi/s$, where n is a positive integer;
- the magnitude is limited— $|\mathbf{k}| < k_c$;
- when $\mathbf{k}_{\parallel} = \mathbf{0}$, there are no surface plasmon modes (which would not be normalizable) and no bulk plasmon modes of type 2 (which would be zero everywhere).

For the cut-off wavevector k_c , we use the result (38) for the homogeneous electron gas. One could argue that a lower cut-off ought to be used for the surface plasmon modes, for which $\omega \approx \omega_p/\sqrt{2}$ when k_{\parallel} is large; however, the cut-off is only expected to be correct to within an order of magnitude, and we use the same value for both sets of plasmons.

5.2. The plasmon Jastrow factor

Having identified the normal modes, we can apply the prescriptions (35) and (36) to construct the Jastrow factor. The resulting two-body term is

$$u_{\text{pl}}(\mathbf{r}, \mathbf{r}') = \frac{e^2}{\hbar\omega_{\text{p}}\epsilon_0 L^2 s} \sum_{\mathbf{k}_{\parallel}} \cos[\mathbf{k}_{\parallel} \cdot (\mathbf{r}_{\parallel} - \mathbf{r}'_{\parallel})] \left[F_{k_{\parallel}}(z, z') + \sum_{k_z} \frac{4}{k^2} \sin k_z z \sin k_z z' \Theta(z) \Theta(s-z) \Theta(z') \Theta(s-z') \right]. \quad (54)$$

The function $F_{k_{\parallel}}$ is defined in appendix A.

Since the density depends only on z , terms with $\mathbf{k}_{\parallel} \neq \mathbf{0}$ do not contribute to the one-body term, and surface plasmon modes are excluded. Assuming once again that the density is constant within the slab and zero outside gives

$$\chi_{\text{pl}}(\mathbf{r}) = \frac{e^2}{\hbar\omega_{\text{p}}\epsilon_0} \sum_{k_z} \frac{4n_0}{k_z^3 s} \sin k_z z (1 - \cos k_z s) \Theta(z) \Theta(s-z). \quad (55)$$

5.3. Approximate analytic solution for a single surface

It is possible to obtain an approximation to u_{pl} by taking the slab width s and the cell size L to infinity, in which case the sums become integrals. The system is no longer a slab but a single surface (at $z = 0$) of infinite extent in the xy -plane. If we also neglect the cut-off k_c , then we can solve the integrals analytically; in this limit, the full plasmon two-body function is

$$u_{\text{pl}}^{\infty}(\mathbf{r}, \mathbf{r}') = \frac{e^2}{4\pi\epsilon_0\hbar\omega_{\text{p}}} \left[\Theta(z)\Theta(z') \left(\frac{1}{|\mathbf{r} - \mathbf{r}'|} - \frac{1}{\sqrt{(z+z')^2 + (\Delta r_{\parallel})^2}} \right) + \frac{\sqrt{2}}{\sqrt{(|z| + |z'|)^2 + (\Delta r_{\parallel})^2}} \right]. \quad (56)$$

The contribution from the bulk plasmons is only relevant when both electrons are inside the electron gas; when the electrons are deep inside, u_{pl}^{∞} tends to the expected homogeneous electron gas form (37). The correlation is boosted for electrons closer to the boundary.

The singularity at $\mathbf{r} = \mathbf{r}'$ is a result of neglecting the cut-off k_c ; it does not appear in the original expressions relevant to a finite slab and cell. In any case, the plasmon theory is not expected to predict electron–electron correlation accurately at short range.

5.4. Cusps: desirable and undesirable

The electronic wavefunction should have a cusp when two electrons lie on top of each other [10]. We impose this condition by introducing u_{cusp} and χ_{cusp} , as indicated in equations (41), (42) and (44). This procedure depends on the unmodified wavefunction being smooth: more precisely, it must be possible to expand this function in a Taylor series about the point $\mathbf{r}_i = \mathbf{r}_j$, irrespective of the positions of the other electrons. Unfortunately, this is not true for the plasmon wavefunction: the problem is that both the bulk and surface plasmon modes have cusps at the slab edges. The functions u_{pl} and χ_{pl} therefore also contain cusps. This is not a problem in the infinite barrier model, because the electrons are then strictly confined within the slab, but it is a problem in the jellium slab.

In fact, the cusps in the plasmon wavefunction create a more serious problem in QMC. These extended gradient discontinuities lead to singularities in the Laplacian which should

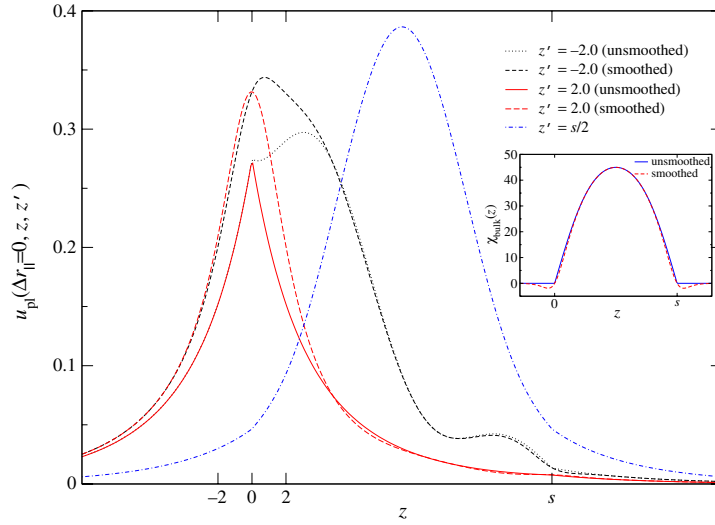


Figure 2. Removing the unphysical slab-edge cusps from u_{pl} (main graph) and χ_{pl} (inset) at the slab boundaries. In the plots of u_{pl} , one electron is fixed while the other is scanned along a line in the z -direction; the x - and y -coordinates are chosen to be the same, so that $\Delta r_{\parallel} = 0$. The smoothed and unsmoothed curves are almost indistinguishable when the electrons are far from the slab edges; the most pronounced difference appears when one electron is just inside the slab edge. These and the following plots were calculated for a cell containing 600 electrons, with $s = 17.64248$ and $r_s = 2.07$ (in Hartree atomic units).

make a finite contribution to the energy expectation value (unlike the point singularities associated with the electron–electron cusps). However, because these points (which constitute a region of zero volume) are never sampled in a QMC simulation, their contribution is missed, and any expectation values involving the Laplacian will not be accurate.

Therefore, in order to achieve proper sampling in QMC, and also to implement the electron–electron cusp conditions correctly, it is necessary to smooth out the plasmon wavefunction: both u_{pl} and χ_{pl} must be modified to have continuous first and second derivatives.

A simple and appealing method of removing the cusps is to modify the piecewise definitions of u_{pl} and χ_{pl} , blurring the boundaries between different regions. The smoothing method which we applied is described in appendix B.

Figure 2 illustrates the effect of removing the undesirable cusps from χ_{pl} and u_{pl} ; some detail is lost when the electrons are close to the slab edges. The complete two-body correlation term, including both u_{pl} and u_{cusp} , is shown in figure 3.

The purpose of the two-body terms is to incorporate correlations into the wavefunction: principally to keep electrons apart. However, a secondary effect (in non-homogeneous systems) is to alter the electron density. In the case of the slab, using only a two-body term forces electrons away from the centre, towards the slab edges; the density spreads out more. This is undesirable, because the initial two-determinant wavefunction usually gives an accurate estimate of the density. The effect of u_{pl} on the electron density is counterbalanced by χ_{pl} ; to counterbalance the effect of including u_{cusp} , we must also include the one-body term χ_{cusp} . We use the prescription (44) to calculate χ_{cusp} . Assuming that the density is constant within the slab, we can perform the integration analytically, as shown in appendix C. The resulting one-body term is plotted in figure 4; the relative size of the correction is small ($\sim 1\%$ of χ_{pl} in the centre of the slab). Fortunately, the correction is cusplless.

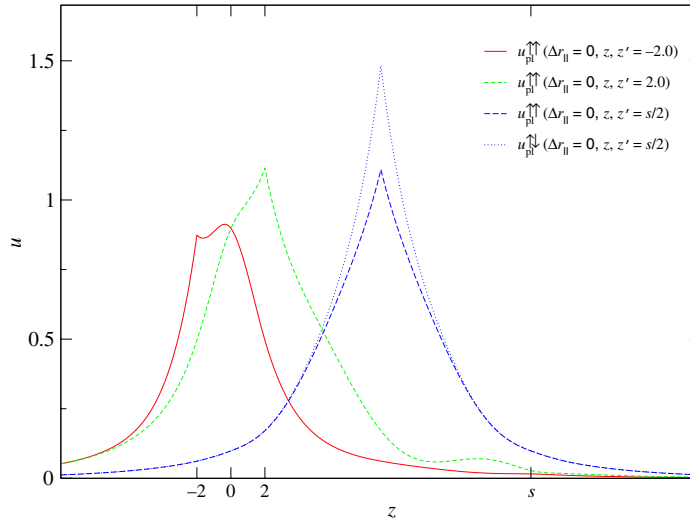


Figure 3. The smoothed plasmon two-body function, to which the correct electron–electron cusps have been added.

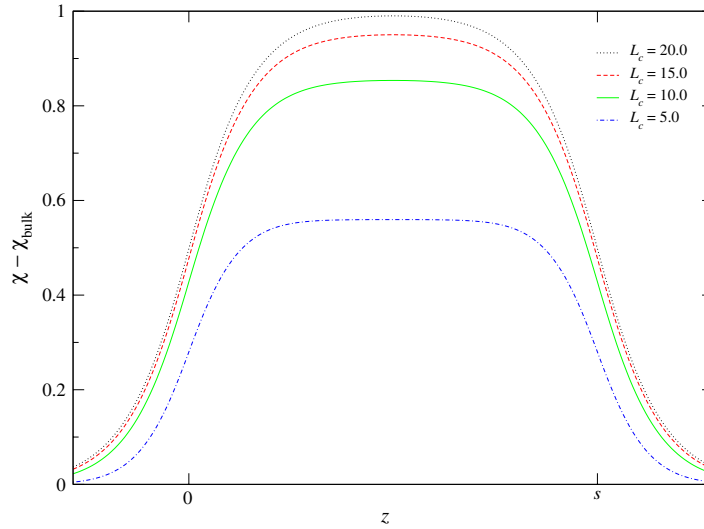


Figure 4. The one-body term χ_{cusp} , for various values of the cut-off distance L_c . As L_c becomes large, the curves tend to a limit, because the decay of u_{cusp} is then dominated by k_c rather than L_c .

6. Results

In order to test the plasmon-derived Jastrow factor for the quasi-2D electron gas, we carried out variational Monte Carlo (VMC) simulations for both the jellium slab and the infinite barrier model. For both systems, a cell containing 600 electrons was used, with the slab width $s = 17.64248$ and density parameter $r_s = 2.07$ (using Hartree atomic units). At this electron density (which corresponds to aluminium), the plasma frequency is $\omega_p \approx 0.6$ and the plasmon reciprocal-space cut-off is $k_c \approx 0.7$.

Using 600 electrons means that the length of side of the cell is $L = 35.5464$; in this relatively large cell the long-range plasmon correlations should be important, whereas in a small cell with $L \sim k_c^{-1}$ the short-range behaviour would be expected to dominate. In addition, it means that $L_c = 5.5$, so that $L_c \gg k_c^{-1}$ and the short-range function u_{cusp} is allowed to decay naturally. As a further check, we also carried out simulations for an even larger system containing 1600 electrons.

The orbitals used to construct the determinant were obtained from LDA calculations. In addition to the VMC energies, it is instructive to compare the electron density profiles generated by the different Jastrow factors:

$$n(z) = \int_{\Omega} |\Psi(\mathbf{r}_1, \dots, \mathbf{r}_N)|^2 \sum_{i=1}^N \delta(z - z_i) d^3r_1 \cdots d^3r_N. \quad (57)$$

During the VMC simulation, we periodically sample the z -positions of the electrons. These coordinates are taken from the distribution with probability density function $n(z)/N$. To see this, consider $P(a < z_1 < b)$ (the probability that the first electron lies in a given z -range):

$$\begin{aligned} P(a < z_1 < b) &= \int_{z_1=a}^b \left(\int_{\Omega} |\Psi(\mathbf{r}_1, \dots, \mathbf{r}_N)|^2 dx_1 dy_1 d^3r_2 \cdots d^3r_N \right) dz_1 \\ &= \int_{z=a}^b \frac{n(z)}{N} dz. \end{aligned} \quad (58)$$

We then reconstruct $n(z)/N$ from the set of sampled points $\{z_i\}$.

6.1. Jellium slab results

In all the density profile plots which follow, we show the LDA profile for reference. This is indistinguishable from the VMC profile when no Jastrow factor is included (as it should be).

First, we investigate the effect of introducing only the homogeneous short-ranged two-body term u_{cusp} . As predicted, the electron density spreads out, coming closer to the homogeneous system; this can be seen in figure 5. However, the effect is small.

The change in electron density brought about by using the plasmon two-body term is much more dramatic, and is illustrated in figure 6. The long-range correlations cause the electron density to be pushed almost entirely into bands outside the original slab. In these regions, u_{pl} is much weaker than in the centre.

The function of the one-body term is to restore the correct electron density. Remarkably, given the dramatic separation observed in figure 6, this is achieved by χ_{pl} ; figure 7 shows the density profile for the wavefunction including the full Jastrow exponent (41).

An important test for the plasmonic wavefunction is to compare it with a wavefunction containing only the short-range electron–electron cusp terms, u_{cusp} and χ_{cusp} . The density is plotted in figure 8, from which it is evident that the original LDA density is almost exactly recovered, except for a small increase in the density very close to the surface. This is an indication that the expression (C.10) for χ_{cusp} , which was not rigorously derived but constructed based on a plausibility argument, works very well for this system.

The results for a larger system of 1600 electrons are almost identical to those for the 600-electron system; table 1 shows the effect of the different Jastrow factors on the VMC energy for the two sizes. The lowest energy is obtained when only the short-ranged part of the Jastrow exponent is used. This is because, in this case, the electron density profile is very close to the (presumably optimal) original LDA profile. The short range of the two-body term means that it disrupts the density less, and there is consequently less work for the one-body function to do.

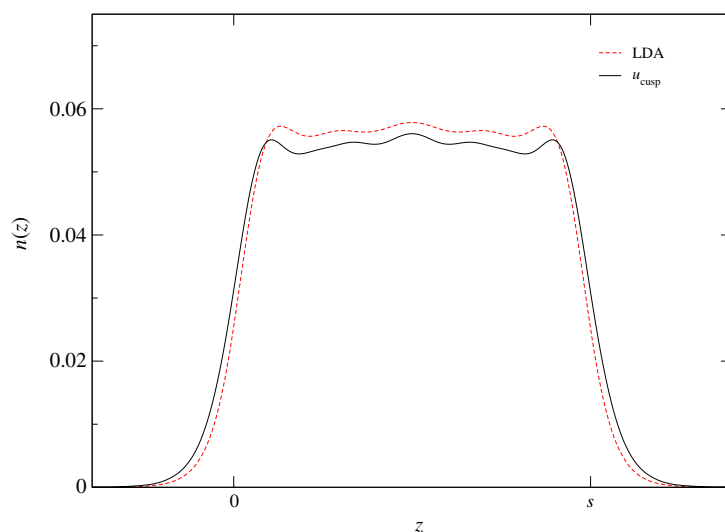


Figure 5. The effect on the electron density of including the homogeneous two-body term u_{cusp} in the Jastrow exponent. The density becomes slightly more homogeneous, with more electrons being pushed into the vacuum regions outside the slab.

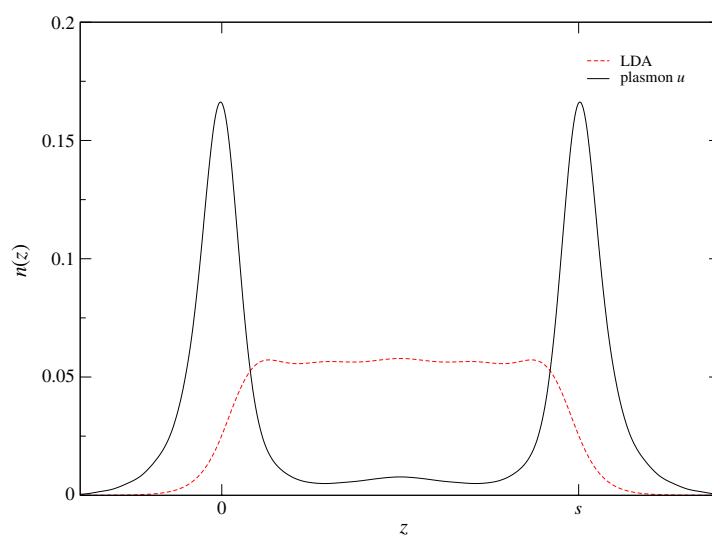


Figure 6. The electron density profile when the plasmon two-body term u_{pl} is included in the VMC wavefunction. The profile is completely different to the original curve, with almost all the electrons now at the slab edges. The change is much more pronounced than when the homogeneous (and short-ranged) u_{cusp} alone is used.

In contrast, the plasmon two-body function is very long ranged, and has an enormous impact on the electron density (as seen in figure 6); the plasmon one-body function is correspondingly large. Although this function comes close to restoring the original density, it is not perfect: this may be due to the way in which the functions have been smoothed, or the fact that the Jastrow factor was derived for an idealized slab of constant density.

These results suggest that having the correct electron density is more important than having the exact two-electron correlation. Up to this point, no optimization has been carried out:

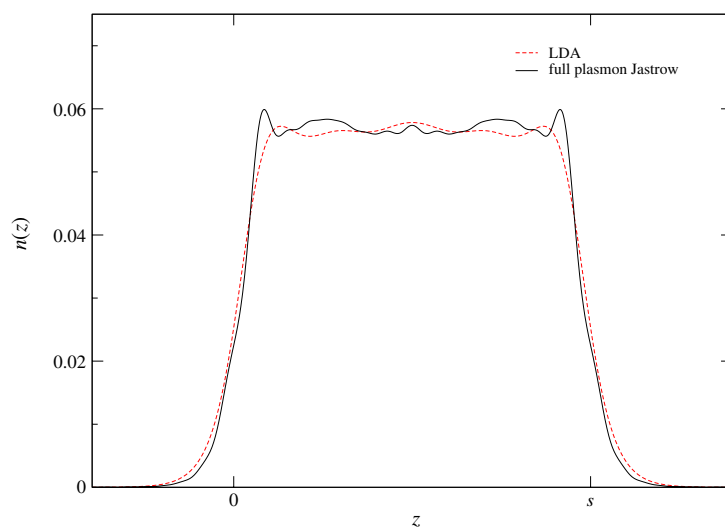


Figure 7. The density profile when the full plasmon Jastrow factor is included in the VMC wavefunction. The result is very close to the original density, although not perfect.

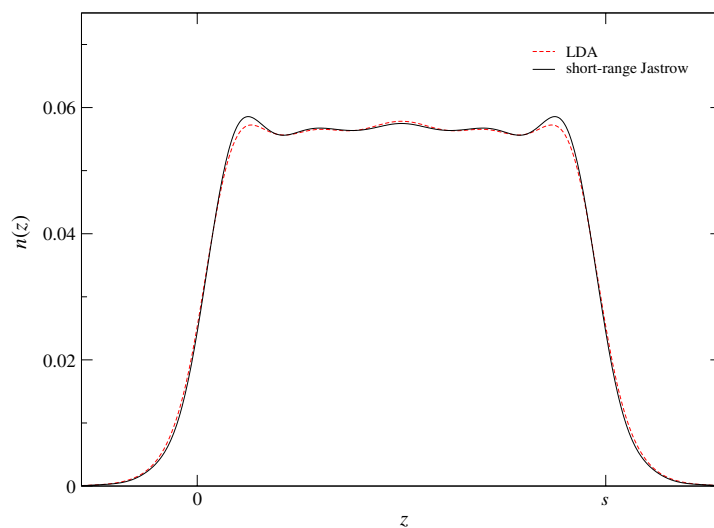


Figure 8. The electron density profile for a Jastrow exponent consisting of only the short-range two-body function u_{cusp} and the corresponding one-body term χ_{cusp} .

all parameters have been calculated in advance, based only on theoretical considerations. To improve the plasmon Jastrow factor, a reasonable approach is to take that predicted by (41) as a starting point, and then to add a small one-body term with adjustable parameters.

6.2. Infinite barrier model results

Although the plasmon Jastrow factor for the unbounded slab performed well, and should provide a good starting point for optimization, the unoptimized form did not improve on the simple short-ranged Jastrow factor, which came closer to maintaining the LDA density and hence generated a lower energy.

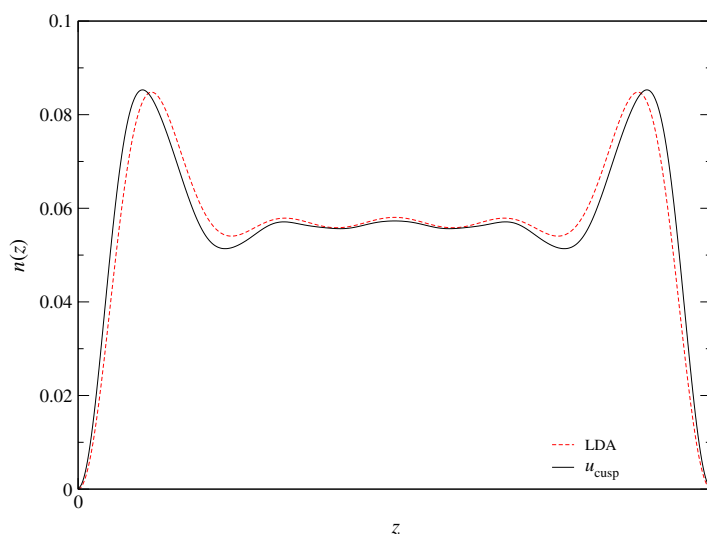


Figure 9. Electron density profile for the bounded slab, with a Jastrow exponent containing only the short-ranged two-body term. The disturbance to the density is small; this is reflected in the VMC energy, which is significantly lower than when using no Jastrow factor.

Table 1. The energy per electron, calculated in VMC, for the unbounded jellium slab. Results for two different cell sizes and various forms of Jastrow exponent are shown. The function u_{pl}^s is the smoothed version of u_{pl} . The ‘full plasmon Jastrow’ refers to a Jastrow exponent of the type described in (41); the ‘short-ranged Jastrow’ uses only u_{cusp} and χ_{cusp} .

Number of electrons in cell	Jastrow exponent used	Energy per electron (mHartree)
600	None	32.5 ± 0.2
	u_{cusp}	12.5 ± 0.1
	$u_{\text{pl}}^s + u_{\text{cusp}}$	3361 ± 3
	Short-ranged Jastrow	6.14 ± 0.07
1600	None	32.9 ± 0.2
	Short-ranged Jastrow	4.8 ± 0.2
	Full plasmon Jastrow	7.95 ± 0.06
	Full plasmon Jastrow	8.4 ± 0.4

The bounded jellium slab is in some ways a more accurate representation of the system for which the plasmon normal modes were derived; electrons are truly confined to the slab, as in the original model. In the bounded jellium slab, it is not necessary to smooth out the cusps at the slab edges, because the determinantal part of the wavefunction already goes to zero here. The smoothing is presumably one of the areas which contribute to the small but significant errors in the Jastrow factor for the unbounded slab; the fact that it is not required for the bounded slab suggests that the results for the plasmon Jastrow factor should be better here.

Figures 9–12 illustrate the electron density profiles for the various different versions of Jastrow factor; the corresponding energies are recorded in table 2.

The effect of including only the short-range two-body term (figure 9) is to reduce the energy and move the electron density away from the centre of the slab; as in the unbounded slab, the change in the electron density is small.

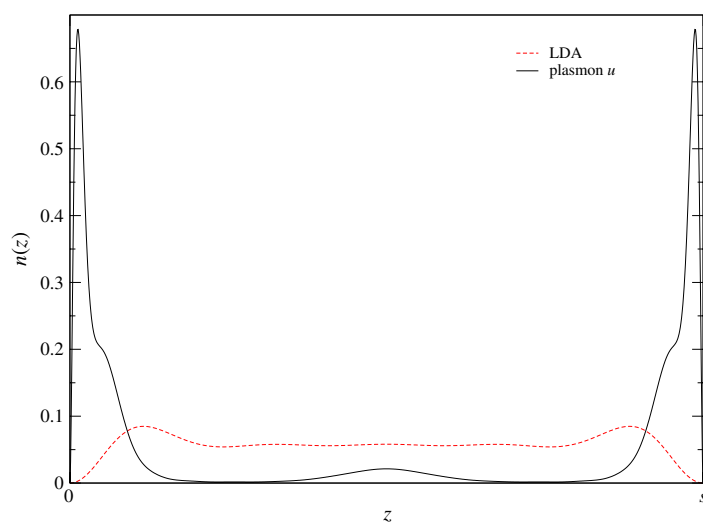


Figure 10. Electron density profile for the bounded slab, with the plasmon two-body term only. The long-ranged correlations alter the density drastically, as in the unbounded slab; electrons are pushed to the slab edges.

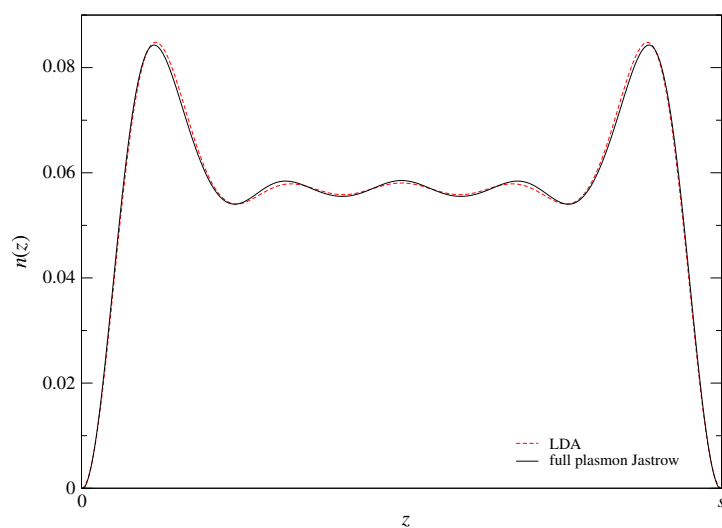


Figure 11. Electron density profile for the bounded slab, with the full plasmon Jastrow factor. The density is very close to the LDA form, and the energy is lower than when using only the short-ranged Jastrow.

Even with the electrons confined to the slab, the plasmon two-body term completely changes the electron density when used without the corresponding one-body function; this is illustrated in figure 10. When the one-body function is applied, the density is very close to the LDA result, as can be seen in figure 11. The correction is better here than in the unbounded slab. Consequently, the energy is lower than that achieved with the full short-ranged Jastrow exponent; the density for the full short-range Jastrow factor, shown in figure 12, is as good as that for the plasmon Jastrow factor, but the energy is higher.

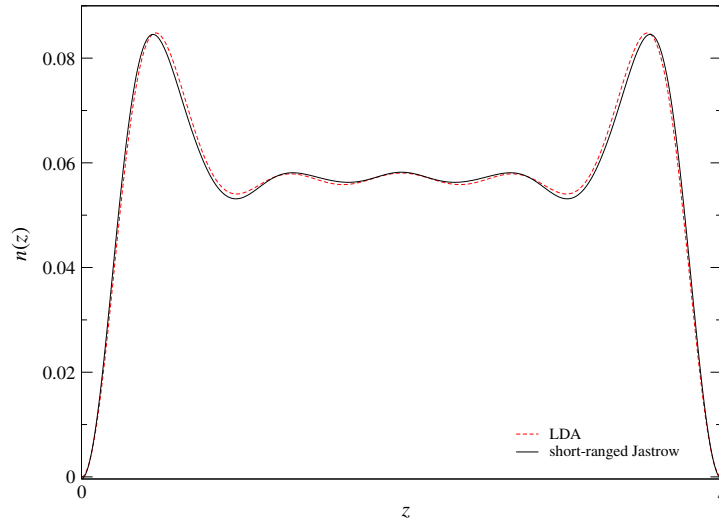


Figure 12. Electron density profile for the bounded slab, with the full short-ranged Jastrow exponent. The LDA density is almost restored, and the energy is lower than when using only u_{cusp} , though not as low as that obtained with the full plasmon Jastrow exponent.

Table 2. The VMC energy per electron for the bounded jellium slab.

Number of electrons in cell	Jastrow exponent used	Energy per electron (mHartree)
600	None	85.9 ± 0.4
	u_{cusp}	62.2 ± 0.3
	$u_{\text{pl}}^s + u_{\text{cusp}}$	8870 ± 70
	Short-ranged Jastrow	58.8 ± 0.2
	Full plasmon Jastrow	55.1 ± 0.1
1600	None	87.9 ± 1.2
	Short-ranged Jastrow	60.1 ± 0.9
	Full plasmon Jastrow	53.3 ± 0.8

7. Conclusions

We have presented an alternative approach to the connection between plasmons and the ground-state wavefunctions of many-electron systems. Our approach reproduces the results of earlier studies [1, 5] while emphasizing the role of the plasmon normal modes; if the normal modes can be obtained, then the wavefunction can be written down immediately.

The plasmon theory is consistent with a wavefunction of the Slater–Jastrow form; the plasmon-derived terms make up part of the Jastrow factor (the part dealing with long-range correlations between electrons). The theory generates both the two-electron correlation function u_{pl} and the single-electron density-correcting function χ_{pl} ; the relationship between these two functions (43) follows the general rule proposed by Malatesta *et al* [6].

We have tested this relationship further, by applying it to our short-range correlation function; we derived χ_{cusp} from u_{cusp} using this formula. The purpose of χ_{cusp} is to counteract the density-altering effect of u_{cusp} , and our results show that this objective is achieved almost perfectly. We therefore strongly recommend the use of relationship (43) as a means of analytically generating the one-body term without the need for optimization; any fine-tuning can be carried out later, starting from a function which is already close to the ideal form.

The plasmon-derived Jastrow factor was successful in reducing the expectation value of the energy beyond the level achieved by the short-range terms alone for the bounded slab, but not for the unbounded one. The bounded slab is perhaps closer to the model system for which the normal modes were derived; more importantly, however, the troublesome gradient discontinuities are not present in the plasmon Jastrow factor for this system because the electrons are kept strictly inside the slab, and the wavefunction does not need to be smoothed. In the unbounded jellium slab, the plasmon one- and two-body terms are no longer perfectly matched; the long-range correlations alter the electron density in a way that is not completely compensated for by χ_{pl}^s . This disturbance to the density means that the energy expectation value actually increases slightly when the plasmon terms are included. In contrast, the plasmon-derived one-body term does a much better job of correcting the electron density in the bounded slab system, and the result is that the expectation value of the energy is reduced.

A better wavefunction could be obtained by including an additional one-body function in the Jastrow exponent, which should be optimized with the aim of lowering the energy or variance, while retaining the long-range plasmon-derived correlations. However, the plasmon terms are computationally costly, and it may be more practical to use only the short-range correlation function, together with the associated one-body term. These can be calculated quickly, and greatly reduce the need for optimizing parameters.

Appendix A. Definition of $F_{k_{\parallel}}$

The contribution of the surface plasmon modes to u_{pl} is obtained by substituting the fields (51) and (52) and the dispersion relation (53) into the prescription (36) for the two-body term. The result is

$$u_{\text{surf}}(\mathbf{r}, \mathbf{r}') = \frac{e^2}{\hbar\omega_{\text{p}\epsilon_0}L^2s} \sum_{\mathbf{k}_{\parallel}} \cos[\mathbf{k}_{\parallel} \cdot (\mathbf{r}_{\parallel} - \mathbf{r}'_{\parallel})] F_{k_{\parallel}}(z, z'). \quad (\text{A.1})$$

The function $F_{k_{\parallel}}$ is defined piecewise in table A.1. The constants used in this definition are

$$\begin{aligned} A_{k_{\parallel}} &= \frac{s\sqrt{2}}{2k_{\parallel}\sqrt{1+e^{-k_{\parallel}s}}} \\ B_{k_{\parallel}} &= \frac{s\sqrt{2}}{2k_{\parallel}\sqrt{1-e^{-k_{\parallel}s}}} \\ C_{k_{\parallel}} &= 1 - e^{k_{\parallel}s} \\ D_{k_{\parallel}} &= 1 + e^{k_{\parallel}s}. \end{aligned} \quad (\text{A.2})$$

Table A.1. The function $F_{k_{\parallel}}(z, z')$. This contains all the z - and z' -dependence of the part of u_{pl} arising from the surface plasmon contribution. The constants $A_{k_{\parallel}}$, $B_{k_{\parallel}}$, $C_{k_{\parallel}}$ and $D_{k_{\parallel}}$ are defined in equation (A.2).

z	z'	$F_{k_{\parallel}}(z, z')$
<0	<0	$e^{k_{\parallel}(z+z'-s)}(-A_{k_{\parallel}}C_{k_{\parallel}} + B_{k_{\parallel}}D_{k_{\parallel}})$
<0	$0 \rightarrow s$	$e^{k_{\parallel}(z+z'-s)}(-A_{k_{\parallel}} + B_{k_{\parallel}}) + e^{k_{\parallel}(z-z')}(A_{k_{\parallel}} + B_{k_{\parallel}})$
<0	$>s$	$e^{k_{\parallel}(z-z')}(A_{k_{\parallel}}C_{k_{\parallel}} + B_{k_{\parallel}}D_{k_{\parallel}})$
$0 \rightarrow s$	$0 \rightarrow s$	$2 \cosh[k_{\parallel}(z+z'-s)](-A_{k_{\parallel}}/C_{k_{\parallel}} + B_{k_{\parallel}}/D_{k_{\parallel}})$ $+ 2 \cosh[k_{\parallel}(z-z')](A_{k_{\parallel}}/C_{k_{\parallel}} + B_{k_{\parallel}}/D_{k_{\parallel}})$
$0 \rightarrow s$	$>s$	$e^{k_{\parallel}(s-z-z')}[-A_{k_{\parallel}} + B_{k_{\parallel}}] + e^{k_{\parallel}(z-z')}[A_{k_{\parallel}} + B_{k_{\parallel}}]$
$>s$	$>s$	$e^{k_{\parallel}(s-z-z')}(-A_{k_{\parallel}}C_{k_{\parallel}} + B_{k_{\parallel}}D_{k_{\parallel}})$

Appendix B. Smoothing the plasmon wavefunction

The piecewise construction of the plasmon wavefunction for the slab system leads to gradient discontinuities at the slab edges. Here, we describe our method for removing these cusps.

For the purpose of illustration, consider an arbitrary function $f(x)$ with the following form near the point $x = x_0$:

$$f(x) = f_1(x)\Theta(x - x_0) + f_2(x)\Theta(x_0 - x). \quad (\text{B.1})$$

A smooth approximation to f is

$$f^s(x) = f_1(x)T(x - x_0) + f_2(x)T(x_0 - x) \quad (\text{B.2})$$

where the smoothing function T has the following properties:

- the value and first and second derivatives are continuous;
- $\lim_{x \rightarrow \infty} T(x) = 1$;
- $T(x) + T(-x) = 1$.

This ensures that as long as f is continuous, the original value of f on the boundary is preserved. A function with these characteristics is

$$T(x) = \frac{1 - \tanh k_c x}{2}. \quad (\text{B.3})$$

This function has a transition region of size $\sim k_c^{-1}$, which is the shortest length-scale available for plasmons with a cut-off of k_c in reciprocal space. We therefore replace the Heaviside functions in the definitions of u_{pl} and χ_{pl} with T and obtain a wavefunction with continuous second derivatives.

Appendix C. Calculating χ_{cusp}

The formula for the one-body term χ_{cusp} is

$$\chi_{\text{cusp}}(\mathbf{r}) = \frac{1}{2} \int_{\Omega} \left[u_{\text{cusp}}(\mathbf{r} \uparrow, \mathbf{r}' \uparrow) + u_{\text{cusp}}(\mathbf{r} \uparrow, \mathbf{r}' \downarrow) \right] \bar{n}(z') d^3 r' \quad (\text{C.1})$$

$$= \left(\frac{m_e e^2}{4\pi \epsilon_0 \hbar^2} \right) \frac{3}{8k_c} \int_{\Omega} \bar{n}(z') e^{-k_c |\mathbf{r} - \mathbf{r}'| - (\mathbf{r} - \mathbf{r}')^2 / L_c^2} d^3 r'. \quad (\text{C.2})$$

The integral in (C.1) is over the cell. However, the factor of $e^{-(\mathbf{r} - \mathbf{r}')^2 / L_c^2}$ in u_{cusp} is designed to ensure that u_{cusp} becomes zero well before $|\mathbf{r} - \mathbf{r}'|$ approaches the size of the cell. Conveniently, this means that the integral may equally well be evaluated over the entire xy -plane. Switching to cylindrical polar coordinates gives

$$\begin{aligned} I &= \int_{\Omega} \bar{n}(z') e^{-k_c |\mathbf{r} - \mathbf{r}'| - (\mathbf{r} - \mathbf{r}')^2 / L_c^2} d^3 r' \\ &= 2\pi \int_{z'=-\infty}^{\infty} \int_{\rho'=0}^{\infty} \bar{n}(z') \exp\left(-k_c \sqrt{\rho'^2 + (z - z')^2} - \frac{\rho'^2 + (z - z')^2}{L_c^2}\right) \rho' d\rho' dz'. \end{aligned} \quad (\text{C.3})$$

There is no dependence on x and y . A change of variables gives

$$I = 2\pi L_c^2 e^{k_c^2 L_c^2 / 4} \int_{z'=-\infty}^{\infty} \int_{p=|z-z'|/L_c + k_c L_c / 2}^{\infty} \bar{n}(z') \left(\frac{p - k_c L_c}{2} \right) e^{-p^2} dp dz', \quad (\text{C.4})$$

and hence

$$\chi_{\text{cusp}}(\mathbf{r}) = \left(\frac{m_e e^2}{4\pi \epsilon_0 \hbar^2} \right) \frac{3\pi L_c^2}{8k_c} e^{k_c^2 L_c^2/4} \int_{z=-\infty}^{\infty} \bar{n}(z') \left\{ \exp \left(- \left[\frac{|z-z'|}{L_c} + \frac{k_c L_c}{2} \right]^2 \right) - \frac{k_c L_c \sqrt{\pi}}{2} \operatorname{erfc} \left(\frac{|z-z'|}{L_c} + \frac{k_c L_c}{2} \right) \right\} dz'. \quad (\text{C.5})$$

This is a general formula which applies when the electron density is a function of z only. If we make the approximation (once again) that \bar{n} is constant within the slab, we then obtain

$$\chi_{\text{cusp}}(\mathbf{r}) = \left(\frac{m_e e^2}{4\pi \epsilon_0 \hbar^2} \right) \frac{3}{16} n_0 L_c^4 \pi \sqrt{\pi} e^{k_c^2 L_c^2/4} \left\{ - \left(\frac{z}{L_c} + \frac{k_c L_c}{2} + \frac{1}{k_c L_c} \right) \operatorname{erfc} \left(\frac{z}{L_c} + \frac{k_c L_c}{2} \right) - \left(\frac{s-z}{L_c} + \frac{k_c L_c}{2} + \frac{1}{k_c L_c} \right) \operatorname{erfc} \left(\frac{s-z}{L_c} + \frac{k_c L_c}{2} \right) \right. \quad (\text{C.6})$$

$$\left. + \left(\frac{z-a(z)}{L_c} + \frac{k_c L_c}{2} + \frac{1}{k_c L_c} \right) \operatorname{erfc} \left(\frac{z-a(z)}{L_c} + \frac{k_c L_c}{2} \right) \right. \quad (\text{C.7})$$

$$\left. + \left(\frac{a(z)-z}{L_c} + \frac{k_c L_c}{2} + \frac{1}{k_c L_c} \right) \operatorname{erfc} \left(\frac{a(z)-z}{L_c} + \frac{k_c L_c}{2} \right) \right. \quad (\text{C.8})$$

$$\left. + \frac{1}{\sqrt{\pi}} e^{-(z/L_c + k_c L_c/2)^2} + \frac{1}{\sqrt{\pi}} e^{-[(s-z)/L_c + k_c L_c/2]^2} \right. \quad (\text{C.9})$$

$$\left. - \frac{1}{\sqrt{\pi}} e^{-[(z-a(z))/L_c + k_c L_c/2]^2} - \frac{1}{\sqrt{\pi}} e^{-[(a(z)-z)/L_c + k_c L_c/2]^2} \right\} \quad (\text{C.10})$$

where

$$a(z) = \begin{cases} 0 & \text{when } z < 0 \\ z & \text{when } 0 < z < s \\ s & \text{otherwise.} \end{cases} \quad (\text{C.11})$$

References

- [1] Bohm D and Pines D 1953 A collective description of electron interactions: III. Coulomb interactions in a degenerate electron gas *Phys. Rev.* **92** 609
- [2] Hammond B L, Lester W A Jr and Reynolds P J 1994 *Monte Carlo Methods in Ab Initio Quantum Chemistry* (Singapore: World Scientific)
- [3] Foulkes W M C, Mitas L, Needs R J and Rajagopal G 2001 Quantum Monte Carlo simulations of solids *Rev. Mod. Phys.* **73** 33
- [4] Ceperley D M 1978 Ground state of the fermion one-component plasma *Phys. Rev. B* **18** 3126
- [5] Gaudoin R, Nekovee M, Foulkes W M C, Needs R J and Rajagopal G 2001 Inhomogeneous random-phase approximation and many-electron trial wavefunctions *Phys. Rev. B* **63** 115115–30
- [6] Malatesta A, Fahy S and Bachelet G B 1997 Variational quantum Monte Carlo calculation of the cohesive properties of cubic boron nitride *Phys. Rev. B* **56** 12201–10
- [7] Landau L D and Lifshitz E M 1997 *Course of Theoretical Physics* vol 1 *Mechanics* (Oxford: Butterworth–Heinemann)
- [8] Raimes S 1972 *Many-Electron Theory* (Amsterdam: North-Holland)
- [9] Doniach S and Sondheimer E H 1998 *Green's Functions for Solid State Physicists* (London: Imperial College)
- [10] Kato T 1957 *Commun. Pure Appl. Math.* **10** 151
- [11] Fahy S, Wang X W and Louie S G 1990 Variational quantum Monte Carlo nonlocal pseudopotential approach to solids: formulation and application to diamond, graphite, and silicon *Phys. Rev. B* **42** 3503–22
- [12] Jackson J D 1999 *Classical Electrodynamics* (New York: Wiley)
- [13] Ritchie R H 1957 Plasma losses by fast electrons in thin films *Phys. Rev.* **106** 874–81
- [14] Ferrell R A 1958 Plasma oscillations in metal films *Phys. Rev.* **111** 1214–21
- [15] Boardman A D 1982 *Electromagnetic Surface Modes* (Chichester: Wiley)